demonstrated by immunofluorescence studies at the exacerbated phase of proteinuria on days 7 – 9 following PA administration. Using semi-quantitative RT-PCR, the mRNA level of nephrin on day 3 was demonstrated to decrease to 60% of the control following a single injection of 200 mg kg^{-1} (16) or 150 mg kg^{-1} (12) PA. However, the mRNA level of nephrin on day 9 was also demonstrated controversially to decrease to 80% of control following a single injection of 100 mg kg^{-1} PA (13). With regards to podocin in PA nephrosis, stable mRNA levels were demonstrated at the time that podocin protein levels decreased (14, 15). Therefore, there are discrepancies between the mRNA level and the protein level of podocin in PA nephrosis.

The aim of this study is to investigate the mRNA and protein levels of nephrin and podocin before the onset of proteinuria in PA nephrosis from day 1 to day 5 following PA administration. The daily profiles of the expressions of nephrin and podocin before the onset of proteinuria will contribute to the elucidation of the mechanism of nephrosis induced by PA.

Materials and Methods

Animals

Thirty male Sprague-Dawley strain rats weighing 150 – 180 g (Saitama Experimental Animal, Saitama) were fed with a basal diet in metabolic cages (TECNIPLAST, Buguggiate, Italy) at room temperature with a 12-h light/dark cycle. Water was given ad libitum.

For the induction of PA nephrosis, 120 mg kg^{-1} of PA (Sigma P7130; Sigma, St. Louis, MO, USA) was dissolved at a concentration of 24 mg ml^{-1} in saline and injected into 15 rats subcutaneously on the first day of the experiment (day 0). Fifteen control rats were injected with the same amount of saline subcutaneously. One to five days following PA administration, three saline-injected rats and three PA-injected rats were weighed and anesthetized with an intraperitoneal injection of 50 mg kg^{-1} pentobarbital, and their kidneys were excised each day. Left kidneys were frozen immediately in liquid nitrogen for extraction of total RNAs. Right kidneys were sliced, embedded in OCT compound, and frozen on liquid nitrogen to prepare frozen sections. Animal handling followed the ethical guidelines of the Kyorin University School of Medicine.

Protein content assay and SDS-PAGE of the urine

Protein in 10 μl of urine was precipitated with 10% trichloroacetate on ice for 30 min and then centrifuged for 15 min at 15,000 rpm. The precipitated urinary proteins were dissolved in 50 μl of distilled water and the protein concentration was determined by BCA protein assay kit (Pierce Biotechnology, Rockford, IL, USA). Urinary excretion of protein was determined from the urinary protein concentration and the volume of urine collected by the metabolic cage. For the quantification of urinary albumin, the precipitated urinary proteins, corresponding to 1/20,000 of daily excretion from three rats, were also separated by SDS-PAGE with 10% polyacrylamide gels and stained with Coomassie Brilliant Blue R-250. The density of 60 kD band was analyzed using NIH image 1.62.

TaqMan real time RT-PCR quantitative system

Total RNA in frozen left kidney was extracted using 10 ml of ISOGEN kit (Nippongene, Tokyo) and homogenized with a POLYTRON homogenizer (PT10/35; KINEMATICA AG, Littau-Lucerne, Switzerland). The crude total RNA was purified with RNase-free DNase using an RNeasy Mini kit (QIAGEN, Valencia, CA, USA). One microgram of the total RNA was used for generating cDNAs by reverse transcription with 2.5 μM random hexamers and TaqMan Reverse Transcription Reagents (Applied Biosystems Japan, Tokyo). For rat nephrin mRNA quantification, primers (rNEF-Q1: 5'-TAATGTGTCTGCGGCCCAG-3' and rNEF-Q1R: 5'-TGTTGGTGTGGTCAGAGCCA-3') and TaqMan probe (rNEF-TAQ1: 5'-CCCTCTTCAAATGCACGGCCACC-3') were synthesized. For rat podocin mRNA quantification, primers (rPodo-Q1: 5'-GGCACAAAGACAGGCC AAA-3' and rPodo-Q1R: 5'-ACTCAGAGGCAGCTT TTTCCC-3') and TaqMan probe (rPodo-TAQ1: 5'-TGC GGGTGATTGCTGCC GAA-3') were synthesized. Real time quantitative PCR was performed from the 0.02 μg cDNA using TaqMan Universal Master Mix and ABI 7700 sequence detector according to the manufacturer's instructions.

Indirect immunofluorescence and confocal microscopy

Frozen kidney slices, embedded in OCT compound, were cut into 4-μm-thick sections and immunostained with anti-rat podocin polyclonal antibody and anti-human nephrin polyclonal antibody. Anti-rat podocin polyclonal antibody was generated against a synthetic peptide corresponding to KAGRGNRGRARPDAGAER (amino acids 28 – 45 of rat podocin). A rabbit was immunized with peptide conjugated with the carrier protein, keyhole limpet hemocyanin (KLH). The peptide-specific IgG fraction was further immunoaffinity-purified. Rabbit polyclonal antibody against the intracellular part of human nephrin (UP3) (8) was used for the immunofluorescence studies of rat nephrin. The kidney sections were incubated with blocking buffer for 1 h at room temperature and then reacted with anti-rat

podocin antibody (1:500) or anti-human nephrin polyclonal antibody (1 μg/ml) in blocking buffer for 60 min at room temperature. After washing three times with PBS-Tween 20, the kidney sections were incubated with Alexa Fluor 488 goat anti-rabbit IgG (1:200; Molecular Probes, Inc., Leiden, Netherlands) for 40 min at room temperature. Following a final washing with PBS, the kidney sections were mounted in 1 mg/ml *p*-phenylenediamine in PBS/glycerol (1:1) to retard laser bleaching and examined by fluorescence microscopy using a confocal laser scanning microscope (GB 200; Olympus, Tokyo).

Western blotting

For Western blotting, three control rats and three PA-injected rats from days 1 to 5 after PA administration were anesthetized, and both of their kidneys were excised. For isolation of glomeruli, minced cortical kidney tissue was scraped on ice-cold sieves of 180-μm pores and sieved through sequential sieves of 180- and 105-μm pores with ice-cold saline. The glomeruli were isolated on the sieve of 65-μm pores. After adding 2 ml of PBS containing protease inhibitors (Complete; Roche Diagnostics KK, Tokyo) to the isolated glomeruli from one rat, the mixture was homogenized in a Potter-Elvehjam homogenizer on ice. The homogenate was centrifuged at 6,000 × *g* for 15 min at 4°C, and the resultant supernatant was centrifuged at 100,000 × *g* for 30 min at 4°C. The precipitate was resuspended with the PBS-containing protease inhibitors as a crude membrane fraction. Protein concentrations of samples were determined with a BCA protein assay kit (Pierce Biotechnology).

Western blotting analysis was performed as follows: 1-μg samples of the crude membrane fraction of glomeruli from the control rat and PAN rats were separated on a 10% polyacrylamide gel by the Laemmli method and then semi-dry blotted on a PVDF filter (Immobilon-P, Millipore Co., Bedford, MA, USA). The blotted filter was shaken for 1 h at room temperature in blocking solution (5% blocking agent of the ECL kit (Amersham Biosciences) in the TBS with 0.02% Tween 20) and then washed three times with washing solution (150 mM NaCl, 10 mM Tris-HCl, pH 7.8, 0.1% Tween 20). The blocked filter was stained overnight at 4°C using primary antibodies in the TBS-T solution containing 1% bovine serum albumin. The detection was performed according to the manufacturer's instructions with the ECL kit (Amersham Biosciences). The intensity of the bands was analyzed using NIH image 1.62.

Data analysis and statistical assessment

The results from the representative experiments are expressed as the mean ± S.E.M. Statistical analyses were performed using the unpaired *t*-test.

Results

Daily profile of body weight and urinary protein content

Figure 1A illustrates the daily profile of body weight in control and PAN rats. The average body weight of PAN rats decreased to 15.8 ± 2.1 g at day 1 after PA administration (n = 15). However, the weight gain of PAN rats was almost the same as that of control rats

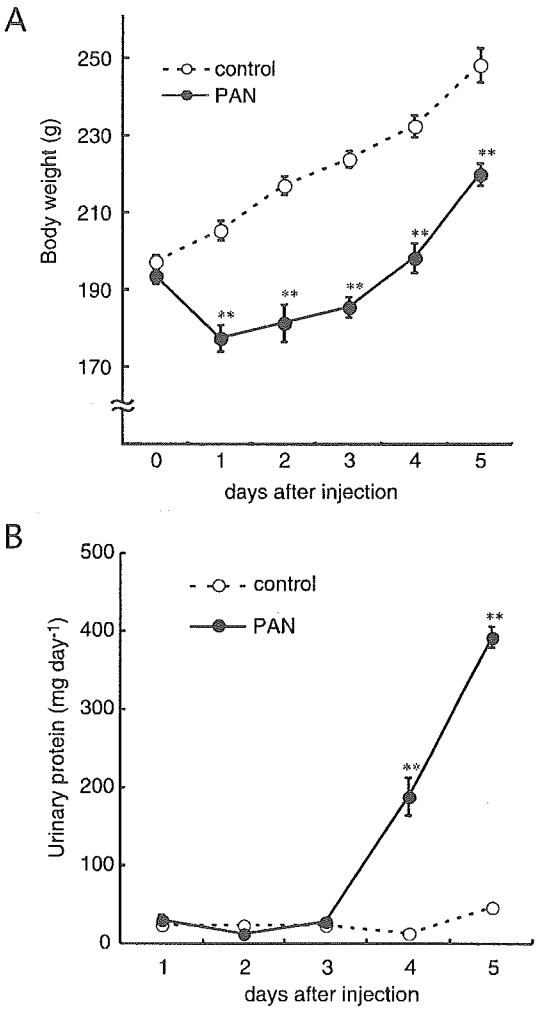

Fig. 1. Daily profile of body weights and urinary protein in PA nephrosis. A) Daily profile of body weights in control and PA-treated rats. Open circles and dotted line represent the body weight of control group rats, which were administered saline on day 0. Closed circles and solid line represent the body weight of the PA nephrosis (PAN) group rats, which were administered PA on day 0. Mean ± S.E.M., n = 15 – 3 $^{**}P<0.01$ *vs* control. B) Daily profile of urinary protein in control and PA treated rats. Open circles and dotted line represent the urinary protein of control group rats. Closed circles and solid line represent the urinary protein of PAN group rats. Mean ± S.E.M., n = 3 $^{**}P<0.01$ *vs* control.

from day 2. This body weight loss of PAN rats indicated an acute toxicity of PA that was apparent for only one day. The average body weight of PAN rats was significantly lower than that of control rats from day 1 to day 5 following PA administration ($P<0.01$, $n=3-15$). Increased body weight due to nephrosis-induced edema was not observed during this experimental period.

Figure 1B indicates the daily profile of urinary protein in control and PAN rats. Male control rats excreted 26.4 ± 3.1 mg protein per day in their urine ($n=15$). A single subcutaneous injection of 120 mg kg^{-1} PA significantly induced massive proteinuria from day 4, as determined from urine collected from days 3 to 4 ($P=0.002$, $n=3$). Urinary protein excretion at day 4 and day 5 after PA administration was 188.2 ± 24.2 mg protein per day and 392.5 ± 13.4 mg protein per day, respectively ($n=3$).

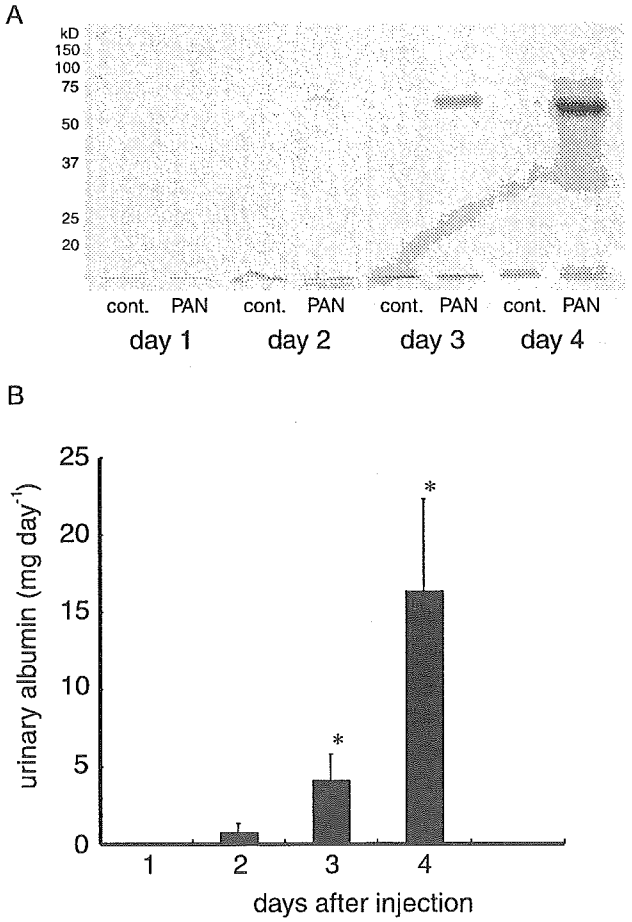

Fig. 2. Daily profile of urinary albumin in PA nephrosis. A) A photograph of SDS-polyacrylamide electrophoresis, which separated urinary proteins from control and PA, treated rats. Urinary proteins were precipitated with 10% trichloroacetic acid and applied 1/20,000 of daily amount. Urinary albumin of PA treated rat was detected as a band of 60-kD protein by staining with Coomassie brilliant blue R-250. There were no protein bands in the urine of control rats. B) Daily profile of urinary albumin in PA treated rats. Mean ± S.E.M., $n=3$ *$P<0.05$ *vs* control.

Daily profile of urinary albumin

Figure 2A shows Coomassie Brilliant Blue-stained urinary proteins separated by SDS-PAGE. The band observed at approximately 60 kD in the urine from the PAN rats was interpreted as urinary albumin. The intensity of the band was analyzed as the urinary albumin content by comparing it with the intensity of bovine serum albumin as a protein standard. The band of albumin was not detected in the urine of control rats nor in the PAN rats at day 1 after PA injection. However, the faint band of albumin could be detected in the urine at day 2 following PA injection. As shown in Fig. 2B, a single subcutaneous injection of 120 mg kg^{-1} PA induced significant albuminuria at day 3, as determined from urine collected from days 2 to 3 ($P=0.04$, $n=3$). Urinary albumin excretion at day 3 and day 4 after PA administration was 4.1 ± 1.7 mg protein per day and 16.4 ± 5.9 mg protein per day, respectively ($n=3$).

Daily profile of the mRNA levels of nephrin and podocin in the kidney

Figure 3 indicates the daily profile of nephrin and podocin mRNA level analyzed with TaqMan real time quantitative PCR. To prevent RNA degradation, each left whole kidney was frozen by liquid nitrogen immediately after excision. TaqMan signal from genomic DNA was eliminated by RNase-free-DNase treatment. To prevent interruption of cDNA elongation, reverse transcription was conducted with random primer. GAPDH mRNA level was used for the internal standard

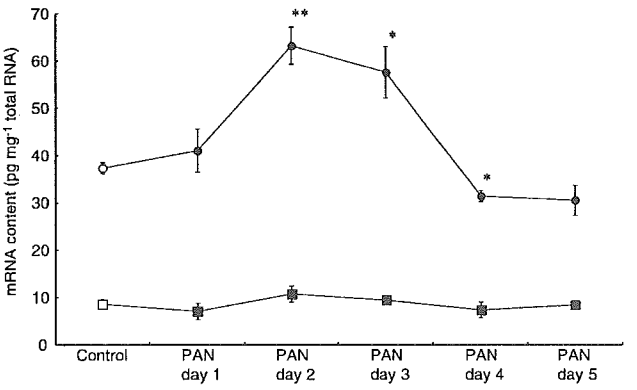

Fig. 3. Daily profile of nephrin and podocin mRNA levels in the kidneys of control and PA treated rats. Open and closed circles represent the amount of nephrin mRNA in 1 mg total RNA from the kidneys of control and PA treated rats, respectively. Open and closed squares represent the amount of podocin mRNA in 1 mg total RNA from the kidneys of control and PA treated rats, respectively. Mean ± S.E.M., $n=3$ **$P<0.01$, *$P<0.05$ *vs* control.

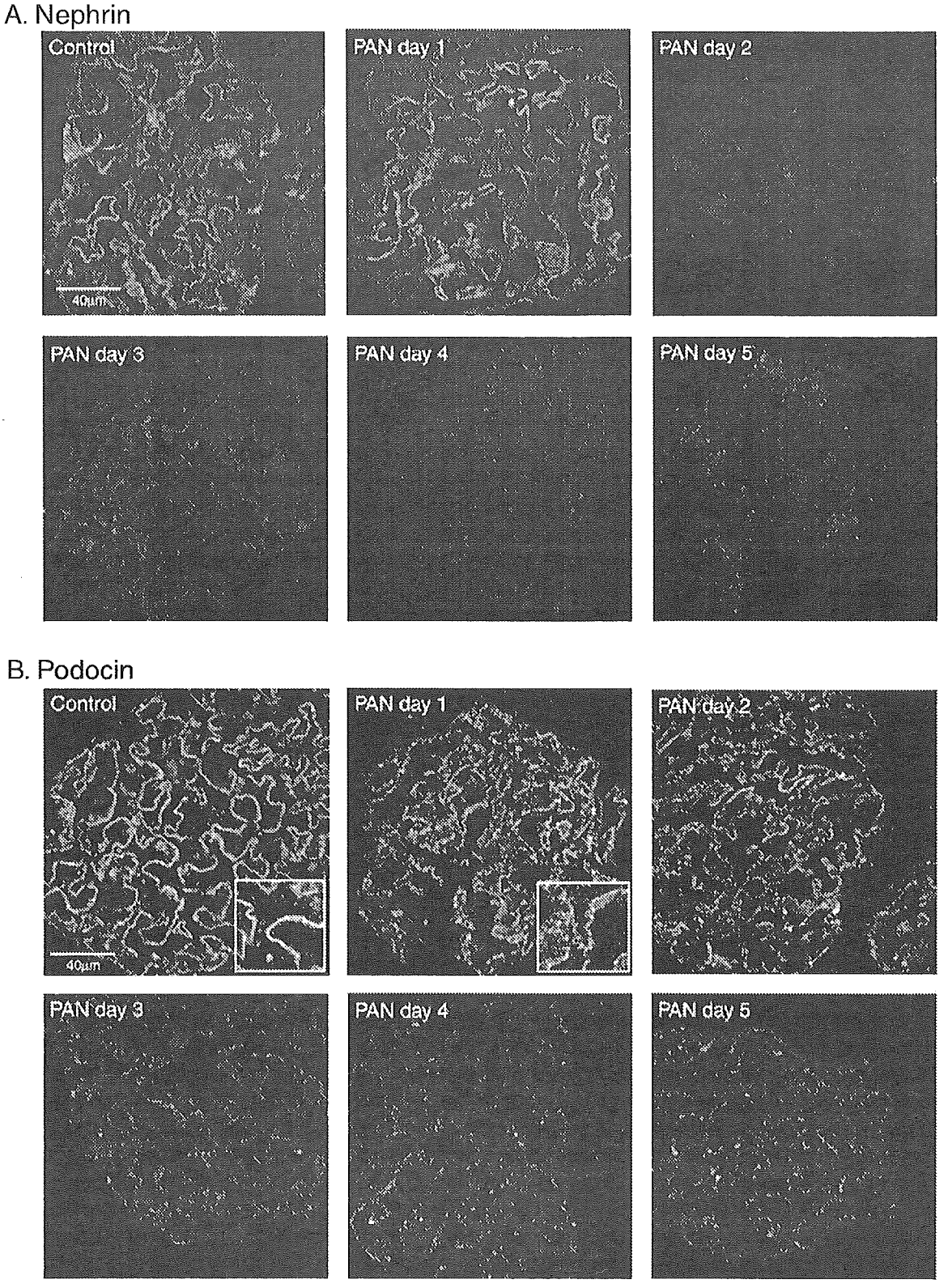

Fig. 4. Daily profile of the localization of nephrin and podocin protein in the glomeruli of control and PA-treated rats. A) Daily profile of nephrin protein localization in the glomeruli of PA-treated rats (n = 2). Normal localization of nephrin in the glomeruli of control rat is indicated in the left-upper panel. All photographs were taken under the same condition for the laser confocal microscope and shown as the same size as indicated by the 40-μm calibration bar at the lower-left corner of the photograph of the control rat. B) Daily profile of podocin protein localization in the glomeruli of PA-treated rats (n = 2). Normal localization of podocin in the glomeruli of control rat is indicated in the left-upper panel. Higher magnifications are shown in the insets.

of sample cDNAs. Nephrin mRNA was calculated to be 44.0 ± 4.7 pg in 1 mg total RNA from the control rat kidney. In PAN rat kidney, nephrin mRNA level was not decreased, but rather was significantly enhanced on days 2 and 3 after PA injection ($P = 0.003$ and 0.026, respectively, n = 3). Nephrin mRNA level was normalized on day 4 after injection and decreased on day 5 ($P = 0.01$). Podocin mRNA was calculated to be 8.7 ± 0.5 pg in 1 mg total RNA from the control rat kidney. In PAN rat kidney, podocin mRNA level was not changed significantly from days 1 to 5 after PA administration.

Daily profile of the protein localizations of nephrin and podocin at the glomeruli

Figure 4A shows the daily profile of nephrin protein localization using indirect immunofluorescence confocal microscopy. The expression pattern of nephrin in PAN rats on day 1 was not different from that of control rats. The intensity of nephrin immunofluorescence started to decline even on day 2 after PA administration, and the decrease in intensity continued until day 5.

Figure 4B shows the daily profile of podocin protein localization using indirect immunofluorescence confocal microscopy. The intensity of podocin immunofluorescence had declined on day 3 after PA administration and the decrease in intensity continued until day 5. Moreover, the localization of podocin in PA nephrosis on day 1 was a dot-like pattern, which was different from the linear pattern of control rats as indicated in the insets.

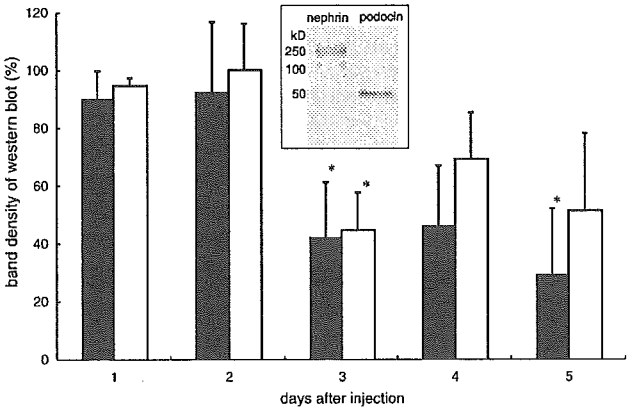

Fig. 5. Daily profile of protein levels of nephrin and podocin in the glomerular crude membrane fraction of PA-treated rats. Closed and open bars represent the percentages of the protein levels of nephrin and podocin in PA-treated rats, respectively. The average percentages of those in control rats were fixed to 100%. The inset demonstrates photographs of Western blotting of the glomerular crude membrane fraction from a control rat using anti-nephrin antibody or anti-podocin antibody. Mean ± S.E.M., n = 3. *$P<0.05$ *vs* control.

Daily profile of protein expression of nephrin and podocin in the glomeruli

Figure 5 shows the daily profile of protein expression of nephrin and podocin in the crude membrane fraction of isolated glomeruli. Similar to Fig. 4, the intensities of the bands of nephrin and podocin decreased significantly at day 3, at which time albuminuria had begun to develop. A photograph of Western blotting using the glomerular crude membrane fraction from a control rat is shown as an inset. Anti-nephrin and anti-podocin antibodies were used as indicated below the photograph. Rat nephrin was detected as a 180-kD strong band, and as a 110-kD faint band, in agreement with previous reports (13). Rat podocin was detected as a single band of 48 kD, almost the same molecular weight as previously reported, 42 kD (14).

Discussion

When PA was administered subcutaneously at 120 mg kg^{-1}, body weight loss was observed at day 1 as an acute toxicity of PA, similar to previous reports (17). Since most of the administered PA was excreted within 8 h (18), the return of body weight gain to normal at day 2 represents recovery from the acute PA toxicity. Although the cause of body weight loss is unknown, the normal gain of body weight indicates that protein synthesis in PAN rats was intact from day 2. Urinary protein was not increased significantly until day 4, with a 3-day latency period as reported previously (19). Urinary albumin appeared at day 3, when rats had already recovered from the acute toxicity of PA.

The protein levels of nephrin and podocin demonstrated by Western blotting decreased at day 3, at the onset of albuminuria. The nephrin and podocin proteins demonstrated by immunofluorescence seemed to disappear at day 2 and at day 3, respectively. Although the disappearance of nephrin (12, 13) and podocin (14, 15) in PA nephrosis has already been reported, in this study, we have demonstrated that these disappearances occurred at approximately the same time as the onset of albuminuria.

We could not detect any significant decrease of the mRNA level of podocin in this study, similar to previous reports (14, 15). Therefore, the decrease of podocin content in the crude membrane of glomeruli was not caused by the decrease of its transcription. Since protein synthesis and the body weight gain of PAN rats were intact from day 2, translation mechanisms also seem to be intact in podocytes on day 3. Moreover, PA is not a protein synthesis inhibitor; therefore, the inhibition of

translation of podocin mRNA was not caused by residual PA in the glomeruli. Although podocin protein does not have a transmembrane domain in its structure, podocin exists in the membrane fraction by interacting with nephrin and Neph1. Therefore, decrease of nephrin protein content in the crude membrane fraction seems to be followed by the decrease of podocin content in it.

Although the podocin localization changed at day 1 from a linear pattern to a dot-like one, the nephrin localization on day 1 was the same as that of the control. Since nephrin is a transmembrane protein localized at the slit diaphragm, no change of nephrin localization on day 1 suggests that the structure of the slit diaphragm was intact on day 1. Thus, the change of podocin localization on day 1 suggests detachment of podocin from nephrin or the dislocation of another interacting protein such as Neph1. The detachment of podocin from nephrin may induce increased turnover of the nephrin molecule.

Although the decrease in nephrin mRNA level was demonstrated at 2 h after PA administration (13), this decrease seems to be an acute toxicity of PA, which has RNA synthesis inhibitor activity (20). The higher nephrin mRNA level on days 2 and 3 in our study is coincident with a previous study, which reported that the nephrin mRNA level increased up to twofold during 4 and 8 weeks of streptozotocin-induced diabetes in rats (21). This increase of nephrin mRNA level suggests an increase of nephrin synthesis to maintain nephrin content in glomeruli under conditions of high nephrin molecule turnover.

The mRNA level of nephrin at day 3 was reported to decrease to 60% of the control by a single injection of 200 mg kg^{-1} (16) or 150 mg kg^{-1} PA (12). Our study also demonstrated that nephrin mRNA levels began to decrease at day 3 and were significantly decreased at day 4. Therefore, PA also induced a decrease in transcription of the nephrin gene around the onset of proteinuria. However, the change in protein-protein interactions of podocin preceded the decrease in nephrin mRNA levels. Kawachi et al. demonstrated a slight decrease in nephrin mRNA levels to 80% of the control on day 9 (13) when proteinuria was sustained. Thus, the elevation of protein turnover of nephrin may be more important to sustained nephrosis than the decrease in nephrin mRNA levels.

On the other hand, the nephrin protein levels demonstrated by immunofluorescence did not change in human glomeruli with minimal change nephrotic syndrome versus control (22). Therefore, the PA nephrosis in rats may not be a close model of human nephrotic syndrome with minimal change. Since the function of Neph1 is thought to be similar to that of nephrin based on the similarity of their structures, the decrease of protein level of Neph1 may induce albuminuria. Thus, the protein level of Neph1 in minimal change nephrotic syndrome and in PA nephrosis must be investigated in the future. Moreover, to clarify the mechanism of nephrosis, gene expression profiles in nephrotic models must be analyzed using cDNA microarray methods (23).

In summary, the protein level of nephrin and podocin decreased at the onset of albuminuria in PA nephrosis. However, the first change induced by PA was the change of podocin localization from a linear pattern to a dot-like one prior to the onset of albuminuria.

Acknowledgment

The authors thank Ms. Akie Toki for her technical assistance. This study was supported in part by Grants-in-Aid from the Ministry of Education, Culture, Sports, Science, and Technology (Numbers 11770048 and 13770048).

References

1 Keane WF. Proteinuria: its clinical importance and role in progressive renal disease. Am J Kidney Dis. 2000;35:S97–S105.
2 Diamond JR, Karnovsky MJ. Focal and segmental glomerulosclerosis following a single intravenous dose of puromycin aminonucleoside. Am J Pathol. 1986;122:481–487.
3 Kestila M, Lenkkeri U, Mannikko M, Lamerdin J, McCready P, Putaala H, et al. Positionally cloned gene for a novel glomerular protein—nephrin—is mutated in congenital nephrotic syndrome. Mol Cell. 1998;1:575–582.
4 Boute N, Gribouval O, Roselli S, Benessy F, Lee H, Fuchshuber A, et al. NPHS2, encoding the glomerular protein podocin, is mutated in autosomal recessive steroid-resistant nephrotic syndrome. Nat Genet. 2000;24:349–354.
5 Kaplan JM, Kim SH, North KN, Rennke H, Correia LA, Tong HQ, et al. Mutations in ACTN4, encoding alpha-actinin-4, cause familial focal segmental glomerulosclerosis. Nat Genet. 2000; 24:251–256.
6 Shih NY, Li J, Karpitskii V, Nguyen A, Dustin ML, Kanagawa O, et al. Congenital nephrotic syndrome in mice lacking CD2-associated protein. Science. 1999;286:312–315.
7 Donoviel DB, Freed DD, Vogel H, Potter DG, Hawkins E, Barrish JP, et al. Proteinuria and perinatal lethality in mice lacking NEPH1, a novel protein with homology to NEPHRIN. Mol Cell Biol. 2001;21:4829–4836.
8 Ruotsalainen V, Ljungberg P, Wartiovaara J, Lenkkeri U, Kestila M, Jalanko H, et al. Nephrin is specifically located at the slit diaphragm of glomerular podocytes. Proc Natl Acad Sci USA. 1999;96:7962–7967.
9 Schwarz K, Simons M, Reiser J, Saleem MA, Faul C, Kriz W, et al. Podocin, a raft-associated component of the glomerular slit diaphragm, interacts with CD2AP and nephrin. J Clin Invest. 2001;108:1621–1629.
10 Sellin L, Huber TB, Gerke P, Quack I, Pavenstadt H, Walz G. NEPH1 defines a novel family of podocin interacting proteins. FASEB J. 2003;17:115–117.

11 Shih NY, Li J, Cotran R, Mundel P, Miner JH, Shaw AS. CD2AP localizes to the slit diaphragm and binds to nephrin via a novel C-terminal domain. Am J Pathol. 2001;159:2303–2308.
12 Luimula P, Ahola H, Wang SX, Solin ML, Aaltonen P, Tikkanen I, et al. Nephrin in experimental glomerular disease. Kidney Int. 2000;58:1461–1468.
13 Kawachi H, Koike H, Kurihara H, Yaoita E, Orikasa M, Shia MA, et al. Cloning of rat nephrin: expression in developing glomeruli and in proteinuric states. Kidney Int. 2000;57:1949–1961.
14 Luimula P, Sandstrom N, Novikov D, Holthofer H. Podocyte-associated molecules in puromycin aminonucleoside nephrosis of the rat. Lab Invest. 2002;82:713–718.
15 Kawachi H, Koike H, Kurihara H, Sakai T, Shimizu F. Cloning of rat homologue of podocin: expression in proteinuric states and in developing glomeruli. J Am Soc Nephrol. 2003;14:46–56.
16 Ahola H, Wang SX, Luimula P, Solin ML, Holzman LB, Holthofer H. Cloning and expression of the rat nephrin homolog. Am J Pathol. 1999;155:907–913.
17 Feigelson EB, Drake JW, Recant L. Experimental aminonucleoside nephrosis in rats. J Lab Clin Med. 1957;50:437–446.
18 Alexander CS, Nagasawa HT, Filbin D. Distribution and excretion of aminonucleoside-8-14C in normal and nephrotic rats. Proc Soc Exp Biol Med. 1962;111:521–526.
19 Hoyer JR, Ratte J, Potter AH, Michael AF. Transfer of aminonucleoside nephrosis by renal transplantation. J Clin Invest. 1972;51:2777–2780.
20 Studzinski GP, Ellem KA. Relationship between RNA synthesis, cell division, and morphology of mammalian cells. I. Puromycin aminonucleoside as an inhibitor of RNA synthesis and division in HeLa cells. J Cell Biol. 1966;29:411–421.
21 Aaltonen P, Luimula P, Astrom E, Palmen T, Gronholm T, Palojoki E, et al. Changes in the expression of nephrin gene and protein in experimental diabetic nephropathy. Lab Invest. 2001;81:1185–1190.
22 Hingorani SR, Finn LS, Kowalewska J, McDonald RA, Eddy AA. Expression of nephrin in acquired forms of nephrotic syndrome in childhood. Pediatr Nephrol. 2004;19:300–305.
23 Izumi Y, Izumiya Y, Shiota M, Yukimura T, Shiojima S, Yamada M, et al. Gene expression profile in experimental mesangial proliferative glomerulonephritis. J Pharmacol Sci. 2004;96:91–94.

Available online at www.sciencedirect.com
SCIENCE DIRECT®
Toxicology 211 (2005) 231–241
TOXICOLOGY
www.elsevier.com/locate/toxicol

CYP1 and AhR expression in 7,12-dimethylbenz[*a*] anthracene-induced mammary carcinoma of rats prenatally exposed to 3,3′,4,4′,5-pentachlorobiphenyl

Shin Wakui [a,*], Kiyofumi Yokoo [a], Hiroyuki Takahashi [b], Tomoko Muto [c], Yoshihiko Suzuki [d], Yoshikatsu Kanai [c], Hiroshi Hano [b], Masakuni Furusato [e], Hitoshi Endou [c]

[a] *Department of Toxicologic Pathology, Azabu University School of Veterinary Medicine, Kanagawa 229-8501, Japan*
[b] *Department of Pathology, Jikei University School of Medicine, Tokyo 105-8461, Japan*
[c] *Department of Pharmacology and Toxicology, Kyorin University School of Medicine, Tokyo 181-8611, Japan*
[d] *Department of Biochemistry, Azabu University School of Veterinary Medicine, Kanagawa 229-8501, Japan*
[e] *Department of Pathology, Kyorin University School of Medicine, Tokyo 181-8611, Japan*

Received 19 January 2005; received in revised form 23 March 2005; accepted 23 March 2005

Abstract

We previously reported the finding that prenatal exposure to a relatively low dose of 3,3′,4,4′,5-pentachlorobiphenyl (PCB126) acted as an enhancing agent for 17-beta-estradiol (E2)-dependent 7,12-dimethylbenz[*a*]anthracene (DMBA)-induced rat mammary carcinoma, while a high dose decreased it. E2 is a known risk factor for mammary carcinoma, and CYP1A1 and 1B1 (CYP1) are the major enzymes catalyzing 2- and 4-hydroxylation of E2, respectively. We investigated the induction of CYP1 and aryl hydrocarbon receptor (AhR) in DMBA-induced mammary carcinoma using female Sprague–Dawley rats whose dams had been treated (i.g.) with 2.5 ng, 250 ng, 7.5 μg of PCB126/kg or the vehicle on days 13–19 post-conception. Immunohistochemical analysis revealed that the mammary carcinoma of the 250 ng group showed a significantly higher number of nuclei expressing estrogen receptor α (ER) and proliferating cell nuclear antigen (PCNA) compared to those of the other groups. Quantitative real-time RT-PCR analysis revealed that the 7.5 μg group showed a significantly higher level of CYP1A1 mRNA, and that the 250 ng group showed significantly higher levels of CYP1B1 mRNA. The level of AhR mRNA was significantly higher in both the 7.5 μg and 250 ng groups. Western blotting analysis was consistent with mRNA changes. It has been revealed that CYP1B1 catalyzes a step in the formation of 4-hydroxylated E2 metabolites, which show quite high mammary carcinogenicity. This study

Abbreviations: PCBs, polychlorinated biphenyls; PCB126, 3,3′,4,4′,5-pentachlorobiphenyl; DMBA, 7,12-dimethylbenz[*a*]anthracene; PBS, phosphate-buffered saline; PCNA, proliferation cell nuclear antigen; ERestrogen receptor α; E2, 17-beta-estradiol; AhR, aryl hydrocarbon receptor; CYP, cytochrome P450

* Corresponding author. Tel.: +81 42 754 1111; fax: +81 42 754 7661.
E-mail address: wakui@azabu-u.ac.jp (S. Wakui).

0300-483X/$ – see front matter
doi:10.1016/j.tox.2005.03.016

indicates that the enhancement of DMBA-induced mammary carcinogenicity in a relatively low PCB126 dose group might partially involve the higher expression of CYP1B1 and AhR in these carcinomas.

Keywords: PCB126; DMBA; CYP1; AhR; Mammary carcinoma; Rat

1. Introduction

Polychlorinated biphenyls (PCBs), dioxin-type chemicals, are used to produce a large number of plastics and other common substances that slowly degrade, allowing PCBs to accumulate in the food chain (Safe and Krishnan, 1995). The hypothesis that PCBs are important cancer-causing agents is supported by studies demonstrating that these chemicals are powerful promoting agents (Hunter et al., 1997; IARC, 1997). Ongoing epidemiologic studies have suggested the carcinogenicity of PCBs in breast carcinoma, but this is still under debate and remains controversial (Safe and Krishnan, 1995).

7,12-Dimethylbenz[*a*]anthracene (DMBA)-induced rat mammary carcinoma, which closely resembles human breast carcinoma (Huggins et al., 1961; Rowlands et al., 2001), has proven to be a useful tool for studying the molecular mechanisms involved in initiation, progression, pathogenesis and prevention of human breast carcinoma (Rowlands et al., 2001).

We previously reported the finding that prenatal exposure to a relatively low dose of 3,3′,4,4′,5-pentachlorobiphenyl (PCB126) enhanced the development of DMBA-induced rat mammary carcinoma, while a high dose decreased it (Muto et al., 2001). Experimental studies have demonstrated that DMBA-induced rat mammary carcinoma is dependent on 17-beta-estradiol (E2) (Huggins et al., 1961). The carcinogenicity of E2 has been primarily attributed to its action as an agonist of the E2 receptor (ER), through which concerted gene regulation controls cellular growth and differentiation in E2 responsive tissues (Nandi et al., 1995; Weinberg, 1996). Recently, increasing evidence for another mechanism of carcinogenicity has focused attention on the catechol E2 metabolites. Two different enzymes are involved in the metabolism of E2: cytochrome P450 1A1 (CYP1A1) and cytochrome P450 1B1 (CYP1B1) (Sasaki et al., 2003). Although aryl hydrocarbon receptor (AhR)-mediated induction of CYP1A1 and 1B1 has been the most frequently studied consequence of AhR activation, AhR expression is also associated with mitogenic responses (Sadhu et al., 1993; Ma and Whitlock, 1996; Bombick et al., 1988; Hushka et al., 1998; Tian et al., 1999). Hence, we performed quantitative real-time RT-PCR and Western blotting analysis for hepatic CYP1A1, 1B1 and AhR in DMBA-induced mammary carcinoma following ingestion of DMBA in female rats whose dams have been exposed to several doses of PCB126 on days 13–19 post-conception.

2. Materials and methods

2.1. Animals, chemicals and treatments

Thirty-two female and eight male 6-week-old Sprague–Dawley (slc) rats (Japan SLC, Shizuoka, Japan) were housed, four per plastic cage, on hardwood-chip bedding in an environment-controlled room on a 12-h light/12-h dark cycle at 22 ± 2 °C and 55 ± 5% relative humidity, with a conventional diet (MF, Oriental Yeast, Tokyo, Japan). All experimental procedures were conducted following approval of the Animal Care and Use Committee of the Azabu University School of Veterinary Medicine. Guidelines set by the National Institute of Health and Public Health Service Policy on the Humane Use and Care of Laboratory Animals were followed at all times. The PCB126 was obtained from AccuStandard Inc., New Haven, CT, and the DMBA was obtained from Tokyo Chemical Industry Co. Ltd., Tokyo, Japan. Seven-week-old rats were housed with four females and a male per plastic cage.

A lifetime tolerable daily intake (TDI) of PCB126 has been reported to range from 10 to 100 pg/kg per day (van den Berg et al., 1998). In this study, three doses of PCB126 were selected using 25 pg/kg/day as the TDI dose (Muto et al., 2001): 10^2-fold of the TDI dose, 10^4-fold of the TDI dose, and 3×10^5-fold of the TDI dose. Groups of eight pregnant rats were treated with 2.5 ng, 250 ng, or 7.5 μg/kg body weight (i.g.) PCB126 or with

an equivalent volume of corn oil (~0.5 ml/animal, i.g.) on days 13–19 post-conception. The offsprings were sexed at birth, and litters were reduced so that each dam was left with eight offsprings (four females/dam). Weaning was carried out on day 21 post-partum. In this study, we considered the group of rats with prenatal exposure to 2.5 ng, 250 ng, or 7.5 μg/kg body PCB126 or with an equivalent volume of corn oil as the 2.5 ng, 250 ng, 7.5 μg or the vehicle group, respectively.

For tumorigenesis experiments, 50-day-old female rats (25 females in each group) received 100 mg/kg DMBA (in corn oil)/kg body weight (i.g.) or (five females in each group) an equivalent volume of corn oil (~0.5 ml/animal, i.g.). In this study, the dose of DMBA was selected following the previous study of Huggins et al. (1961). Rats were palpated everyday for mammary tumors until they were 150 days old. In each group, the cumulative number of tumor masses was calculated by each day's palpation of rats. Samples of the mammary tumors were obtained from rats under deep anesthesia with diethyl ether. Representative sections of each tumor were fixed in 10% phosphate-buffered formalin and routinely processed for hematoxylin–eosin staining. Pathological diagnoses of the mammary lesions were classified as described previously (Russo and Russo, 2000). In addition, other representative sections were frozen without fixation and stored at −80 °C.

2.2. Chemical analysis

Analysis for PCB126 was carried out following the alkaline alcohol digestion method (Tanabe et al., 1987). Aliquots of homogenized rat mammary tumor samples (2 g) were refluxed in 1N KOH-ethanol solution for 1 h. The PCB126 thus extracted into ethanol was transferred to 100 ml of hexane by shaking in a separating funnel. Subsequently, the hexane layer was concentrated and purified by passing it through 1.5 g of silica gel (Wako gel S-1, Wako Co. Ltd., Osaka, Japan) packed in a glass column (10 mm inside diameter × 200 mm length). PCB126 was eluted with 200 ml of hexane at an elution rate of one drop per second. The eluate was concentrated to 5 ml in a Kuderna–Danish concentrator and further purified with 5% fuming sulphuric acid. All samples were injected into a gas chromatograph–mass spectrometer (GC–MS: Shimadzu 9020 DF with an SCAP-1123 data system, Shimadzu Co. Ltd.) equipped with an electron-impact ion-source and moving needle-type injection system for the determination and identification of PCB126. The column consisted of a 0.23 mm inner diameter × 30 m length glass capillary, coated with silicon. Operating conditions of the GC–MS were as follows: column oven temperature was programmed to rise from 190 to 250 °C at 0.5 °C min^{-1}; injector and ion-source temperatures were kept at 250 and 280 °C, respectively. PCB126 was determined by selected ion monitoring at *m/z* 326. The carrier flow of helium was controlled at 0.6 ml min^{-1}.

2.3. Immmuhistochemical analysis

Immunohistochemical analysis for the estrogen receptor α (ER) and the proliferating cell nuclear antigen (PCNA) was performed using avidin–biotin complex (ABC) method. After deparaffinization, 4 μm-thick sections were treated sequentially with 0.3% H_2O_2 for 10 min, and then blocked with 10% goat or horse serum in PBS for 20 min. On thawing, fixed sections were rinsed in PBS and treated with primary antibodies of mouse anti-ER (6F11; Novocastra Laboratories Ltd., Newcastle, UK; diluted 1:100) and mouse anti-PCNA (Novocastra Laboratories Ltd., Newcastle, UK; diluted 1:50). Bound IgG was detected with biotinylated goat anti-rabbit IgG (Vector Lab., Burlingame, CA; diluted 1:100) followed by ABC–peroxidase (Vector Lab., Burlingame, CA) and diaminobenzidine (Sigma, St. Louis, MO). Sections were then counterstained with hematoxylin. As a negative control, unimmunized rabbit serum was substituted for the primary antibody. The numbers of PCNA- or ER-positive cells were measured at random in > 300 cells per section, and the indexes were expressed as percentage values.

2.4. Real-time quantitative RT-PCR analysis

Mammary gland tumor samples were fixed in formalin for histological examination and snap frozen and stored at −80 °C prior to RNA isolation.

Tubulopapillary adenocarcinoma, the major type of carcinoma induced by DMBA in SD rats (Shan et al., 2002), was selected for real-time quantitative RT-PCR analyses in order to avoid the possible variation in expression arising from histologically different tumor subtypes. For each RNA sample, 100 ng was used as the template for first-strand cDNA synthesis

using a TaqMan® Reverse-Transcription kit, following the RT-PCR manufacturer's two-step protocol (PE Applied Biosystems, Foster City, CA). Controls included for each reaction were the RNA sample without reverse transcriptase (RNA-RT) and no RNA with reverse transcriptase (no RNA + RT). The conditions of final reaction for reverse-transcription were as follows: 1× TaqMan RT buffer; 5.5 mM $MgCl_2$; 500 μM dATP, dGTP, and dCTP; 1 mM dTTP; Random Hexamers 0.25 μM; 1.25 U/μl MuLV reverse transcriptase and 0.4 U RNase inhibitor (PE Applied Biosystems, Foster City, CA). Quantitative analyses of target gene (CYP1A1, CYP1B1, and AhR) mRNA expression were performed by real-time quantitative PCR using the ABI Prism 7700 Sequence Detection System (PE Applied Biosystems, Foster City, CA) with TaqMan chemistry and probe. The TaqMan probes and primers for target genes were assay-on-demand gene expression products (PE Applied Biosystems, Foster City, CA) and oligonucleotides with fluorescent reporter and quencher dyes attached (Table 1). Optimal primer, probe and cDNA concentrations were determined in a separate set of experiments to insure that both target gene and GAPDH fragments were amplified with equal efficiency. PCR reactions were performed with first-strand cDNA synthesis (2 μl) from each sample, a Universal PCR Master Mix kit (PE Applied Biosystems, Foster City, CA), 250 nM TaqMan probe, 0.16 U of AmpErase UNG (uracil *N*-glycosylase) and 900 nM forward-reverse primers of the target gene and GAPDH. Three measurements per sample were performed in each of two independent experiments. Results were analyzed with the ABI Sequence Detector software version 1.7 (PE Applied Biosystems, Foster City, CA). For relative quantification of target gene expression, the standard curve method was applied. The calibrated standard curve of each target gene cDNA and GAPDH amplification plots were examined at five different dilutions (containing 100, 50, 25, 10, or 5 ng) of total RNA samples that were obtained from each PCR product using a TOPO II TA Cloning Kit (Invitrogen, Carlsbad, CA) following the manufacturer's recommendations. The normalized target gene value was determined by dividing the average target gene value by the average GAPDH value. The standard deviation (S.D.) of the quotient is calculated from the S.D. of the target gene and GAPDH using the following formula:

$$CV = \frac{\text{S.D. of the quotient}}{\text{mean value of the quotient}}$$

$$(CV)^2 = (CV_1)^2 + (CV_2)^2$$

$$CV_1 = \frac{\text{S.D. of target gene value}}{\text{mean of target gene value}}$$

$$CV_2 = \frac{\text{S.D. of GAPDH value}}{\text{mean of GAPDH}}$$

The normalized target gene value is a unitless number that can be used to compare the relative amount of the target gene in different samples. One way to make this comparison is to designate one of the samples as a calibrator. In this study, the carcinoma of the vehicle group was designated as the calibrator, and the average target gene value was divided by the average calibrator value according to the manufacturer's instructions for quantification of relative gene expression (User Bulletin #2; P/N 4303859, pp. 3–30, 36).

Table 1
ID numbers of TaqMan probes and primers (assay-on-demand gene expression products) for real-time quantitative RT-PCR

Gene	ID
CYP1A1	Rn0048721_ml
CYP1B1	Rn00564055_ml
AhR	Rn00565750_ml

Applied biosystems supplied assay-on-demand gene expression products.

2.5. Western blotting analysis

Rat carcinoma tissues using real-time quantitative RT-PCR analyses were homogenized in 50 mM Tris–HCl, 150 mM KCl (pH 7.4), 1% Triton X-100 and 0.25 mM phenylmethylsulfonyl fluoride (PMSF) and centrifuged at 8000 × *g* for 30 min at 4 °C. The supernatant obtained was centrifuged at 100,000 × *g* for 90 min at 4 °C. The pellet was suspended in 50 mM Tris–HCl (pH 7.4), 1% Triton X-100 and 1 mM PMSF, and the protein concentrations were determined with a bicinchonic acid protein assay reagent kit (Pierce, Rockford, IL) with bovine serum albumin as a standard. Microsomal samples were subjected to electrophoresis on a 10% SDS polyacrylamide gel using 10 μg of microsomes. The proteins were transferred for 2 h to a ni-

trocellulose membrane that was blocked by immersing it in 5% non-fat dried milk in phosphate-buffered saline with 0.1% (v/v) Tween 20 (PBS-T). Western blot analysis was performed using anti-rat-CYP1A1 (Affiniti Res., Exeter, UK), anti-rat-CYP1B1 (BD Gentest, San Jose, CA), or anti-AhR (H-211) (Santa Cruz, CA) antibodies. CYP1A1, CYP1B1 and AhR antibodies were diluted to 1:1000, 1:500 and 1:1000, respectively, in PBS-T and incubated for 1 h at room temperature on an orbital shaker. After being washed three times with PBS-T, they were incubated with a 1:2500 dilution of horseradish peroxidase-conjugated anti-rabbit antibody (Amersham Biosciences, Piscatway, NJ) for 1 h on an orbital shaker. After being washed three times with PBS-T, the membranes were detected using the ECL Plus Western Blotting Detection System (Amersham Biosciences, Buckinghamshire, UK).

2.6. Statistical analysis

For each set, the mean value, standard deviation and standard error of the mean were calculated and compared using Scheffé's *F*-test or chi-square test with the computer statistical analysis program StatView-J 5.0 (Abacus Concepts, Cary, NC).

3. Results

3.1. Body and liver weight, and sexual maturation

Prenatal PCB126 treatment of dams resulted in offspring with body weights at the age of 50 days was practically identical in the vehicle controls and the three dosage groups (Table 2). Endometrial or vaginal hypoplasias were not histologically observed in any group (data not shown). Vaginal opening as evidence of sexual maturity occurred in the 7.5 μg and the 250 ng groups at the age of 36 days, while in the 2.5 ng and the vehicle group it occured at 34 days. The estrous cycle in each group was not investigated.

Table 2
Body and liver weights of 50-day-old female rats after prenatal PCB126 exposure

Group	Body weight (g)	Liver weight (g)
7.5 μg	240.40 ± 5.02	10.70 ± 0.19
250 ng	242.15 ± 3.88	11.94 ± 0.19
2.5 ng	243.68 ± 4.76	10.70 ± 0.30
Vehicle	245.95 ± 8.15	11.66 ± 0.88

Values represent mean ± S.E.M. Scheffé's *F*-test, NS.

Table 3
Incidence of DMBA-induced mammary tumors of rats after prenatal PCB126 exposure

Group	No. of rats	No. (%) of rats with tumor
7.5 ug	25	16 (64%)*
250 ng	25	23 (92%)
2.5 ng	25	21 (84%)
Vehicle	25	22 (88%)

* Chi-square test, $p < 0.05$.

3.2. Tumorigenesis

The incidence of DMBA-induced mammary tumor was significantly lower in the 7.5 μg group, while in the other groups it did not show significant differences from the vehicle group (Table 3). The cumulative tumor development of the 7.5 μg group was the lowest, that of the 250 ng group was the highest and that of the 2.5 ng group was similar to that of the vehicle group (Fig. 1). All DMBA-induced mammary tumors were histologically diagnosed as adenocarcinomas, the majority of them were the tubulopapillary adenocarcinoma type, and the histological type of the mammary carcinoma was similar in all groups (Table 4). The number of the tumor masses in each group of 25 rats is shown in Table 4. At autopsy, there were no nodules or tumor masses in the liver in any of the rats used (data not shown).

Table 4
Histopathological types of DMBA-induced mammary tumors of rats after prenatal PCB126 exposure

Group	Total[a]	Adenocarcinoma	
		Tubulopap.	Comedo-cribri.
7.5 ug	41	30 (76.9%)	11 (28.2%)
250 ng	82	61 (79.2%)	21 (27.3%)
2.5 ng	58	46 (79.3%)	12 (20.7%)
Vehicle	53	43 (81.1%)	10 (18.9%)

Tubulopap.: tubulopapillary type, Comedo-cribi.: Comedo-cribiform type. Chi-square test, NS.

[a] Total number of mammary tumors results are obtained by screening sample from all rats.

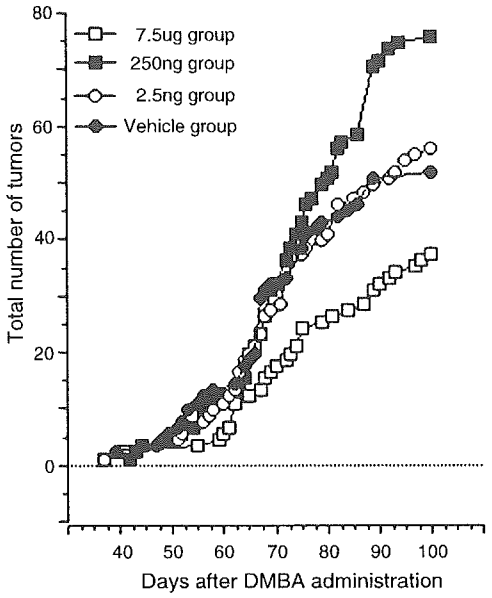

Fig. 1. The time course of tumor appearance showing the effects of prenatal PCB126 exposure on DMBA-induced rat mammary tumorigenesis. Each point represents the total number of palpable mammary tumors in each group of 25 rats. The rate of tumor appearance of the 7.5 μg group was lower than that of other groups, that of the 250 ng group was the highest, and that of the 2.5 ng group was similar to that of the vehicle group.

3.3. Concentration of PCB126 in mammary carcinoma

The concentration of PCB126 in the mammary carcinomas of the 7.5 μg group was not three-fold, but rather four-fold higher than in the 250 ng group, which did not show significant differences from the 2.5 ng and the vehicle group (Table 5).

Table 5
Concentration of PCB126 in DMBA-induced mammary tumors of rats after prenatal PCB126 exposure

Group	
7.5 μg	3.07 ± 0.68**
250 ng	0.71 ± 0.59
2.5 ng	0.36 ± 0.68
Vehicle	0.30 ± 0.62

Values represent mean ± S.E.M. ng/g.
** Scheffé's F-test, $p < 0.01$.

3.4. Immunohistochemical analyses for ER and PCNA

Many cellular nuclei of the mammary carcinoma were immunohistochemically positive for ER and PCNA (Fig. 2). Significantly higher labeling indexes for ER and PCNA were observed in the mammary carcinoma of the 250 ng group, and the other groups showed indexes similar to each other (Fig. 3).

3.5. Quantitative RT-PCR for CYP1A1, CYP1B1 and AhR mRNA

The expressions of CYP1A1 mRNA, CYP1B1 mRNA and AhR mRNA in the mammary carcinomas were analyzed by real-time quantitative RT-PCR. The expression of CYP1A1 mRNA was significantly higher in the mammary carcinoma of the 7.5 μg group compared to that of the other groups (Fig. 4). The expression of CYP1B1 mRNA was significantly higher in the mammary carcinomas of the 250 ng group than that in the other groups (Fig. 4). The expression of AhR mRNA was significantly higher in the mammary carcinomas of both the 7.5 μg and 250 ng groups than that in the other groups (Fig. 4).

3.6. Western blotting for CYP1A, CYP1B1 and AhR

Western blotting analysis revealed that the protein expressions were qualitatively consistent with the patterns observed for CYP1A1 mRNA, CYP1B1 mRNA and AhR mRNA (Fig. 5).

4. Discussion

Direct-tumor promoting effects of PCBs by various mechanisms might occur throughout carcinogenesis, even though the precise mechanism remains controversial (Safe and Krishnan, 1995; Tharappel et al., 2002; Borlak et al., 2003). The breast carcinogenicity of E2 has been primarily attributed to its action as an agonist of the ER (Henderson et al., 1991; Nandi et al., 1995; Weinberg, 1996). Our previous study revealed that prenatal exposure to 250 ng PCB126/day (a relatively low dose of PCB126) from days 13 to 19 post-conception enhanced DMBA-induced rat mammary carcinoma,

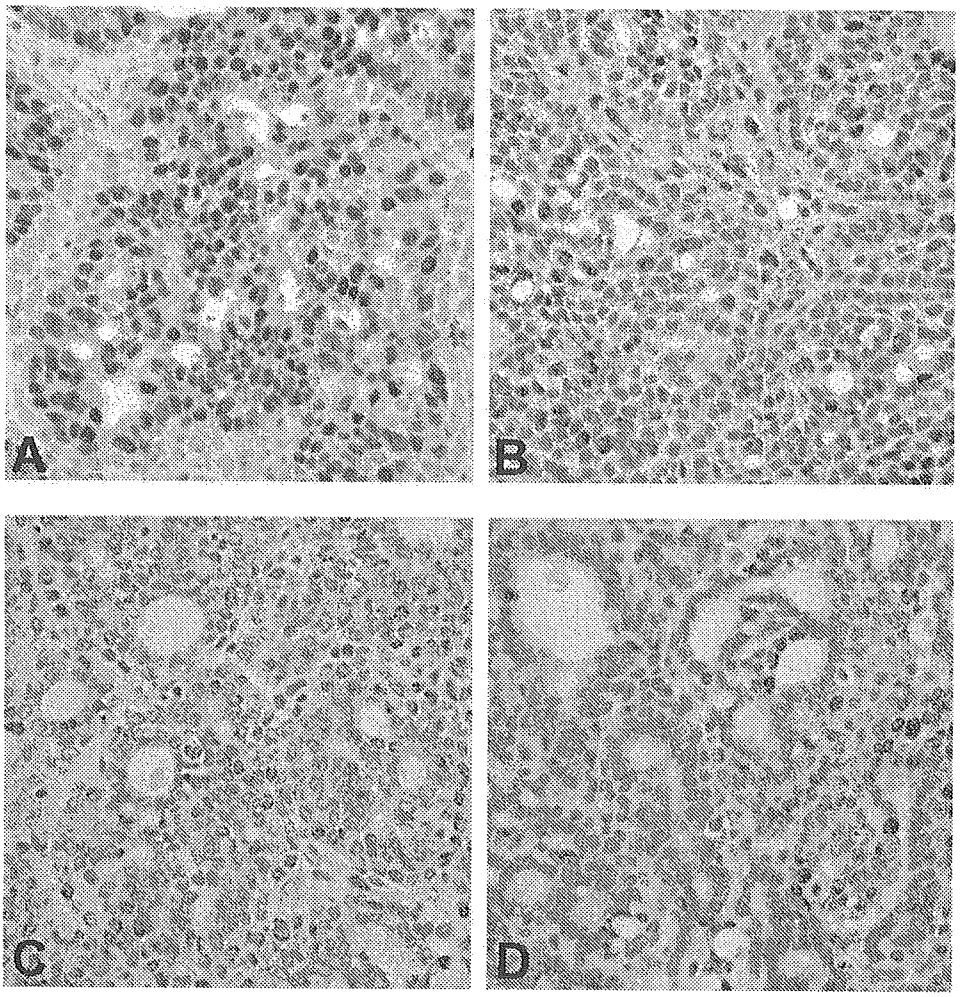

Fig. 2. Representative immunohistochemical analyses for ER (A, B) and PCNA (C, D) of DMBA-induced rat mammary carcinomas after prenatal exposure to PCB126. A number of ER- and PCNA-positive nuclei were observed in the 250 ng group (A: ER, C: PCNA); a small number of them was observed in the 7.5 μg group (B: ER, D: PCNA). ABC method, Mayer's hematoxylin counterstain; 100×.

while a high dose decreased it (Muto et al., 2001). This study confirmed our previous study: the cumulative tumor development of the 250 ng group was the highest, and the incidence of DMBA-induced mammary tumor and the cumulative tumor development were significantly lower in the 7.5 μg group (Muto et al., 2001). Moreover, it was revealed that the DMBA-induced mammary carcinoma in the 250 ng group showed significantly higher ER expression with higher cellular proliferative activity than the other groups.

Increasing evidence of another mechanism of carcinogenicity has focused attention on the catechol E2 metabolites from monohydroxylation reactions (Dwivedy et al., 1992; Liehr et al., 1995). Higher 4-hydroxylated E2 (4OH-E2) concentration has been measured in tumors of the human breast (Furth et al., 1956; Henderson et al., 1991; Lemon et al., 1992; Liehr et al., 1995; Weiss et al., 1996; Newbold and Liehr, 2000). Many studies have reported that 4OH-E2 displays a strong mammary genotoxicity and carcinogenicity (Han and Liehr, 1994; Hayes et al., 1996; Newbold and Liehr, 2000; Sasaki et al., 2003), although it is not known if this function is physiological (Safe and Krishnan, 1995; Cavalieri et al., 2002).

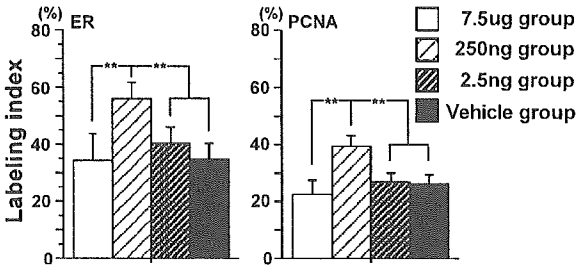

Fig. 3. PCNA and ER labeling index of DMBA-induced rat mammary carcinomas after prenatal exposure to PCB126. The ER and PCNA labeling index of the 250 ng group was significantly higher, and the other groups showed similar indexes. Values represent mean ± S.D. (**) Scheffé's F-test, $p < 0.01$.

4OH-E2 can directly damage DNA, proteins and lipids through the generation of reactive free radicals by the reductive–oxidative cycling of these catechol estrogens between their semiquinone and quinone forms, and by their oxygenated quinone metabolites and depurinating DNA adducts (Dwivedy et al., 1992; Han and Liehr, 1994; Liehr et al., 1995). Moreover, 4OH-E2 binds to ER and shows an estrogenic effect (Tang et al., 1997; Thenot et al., 1999). One step in the formation of 4OH-E2 is catalyzed by CYP1B1 (Hayes et al., 1996; Yager and Liehr, 1996; Mobley et al., 1999; Schumacher et al., 1999; Cavalieri et al., 2002). The predominance of CYP1B1 mRNA and protein is observed in several human breast carcinomas (Merchant et al., 1993; McKay et al., 1995; Huang et al., 1996; Murray et al., 1997). Thus, it has been strongly suggested that 4OH-E2 causes breast and mammary carcinogenesis, and CYP1B1 was implicated as a key physiological regulator in this process (Han and Liehr, 1994; Li et al., 1995; Walker et al., 1999; Newbold and Liehr, 2000; Sasaki et al., 2003). In this study, the 250 ng group showed enhancement of DMBA-induced mammary carcinogenicity, and their mammary carcinomas showed significantly higher expression of CYP1B1 compared to those of the other groups. It seems that the mechanism for enhancement of DMBA mammary carcinoma in the 250 ng group might partially involve the higher expression of CYP1B1 in these carcinomas.

The specific response to exposure to PCBs is an AhR-mediated higher induction of CYP1 (Walker et al., 1999). In this study, the phenomenon of a higher levels CYP1B1 observed in the 250 ng group might be caused by the biological facts that an increase in

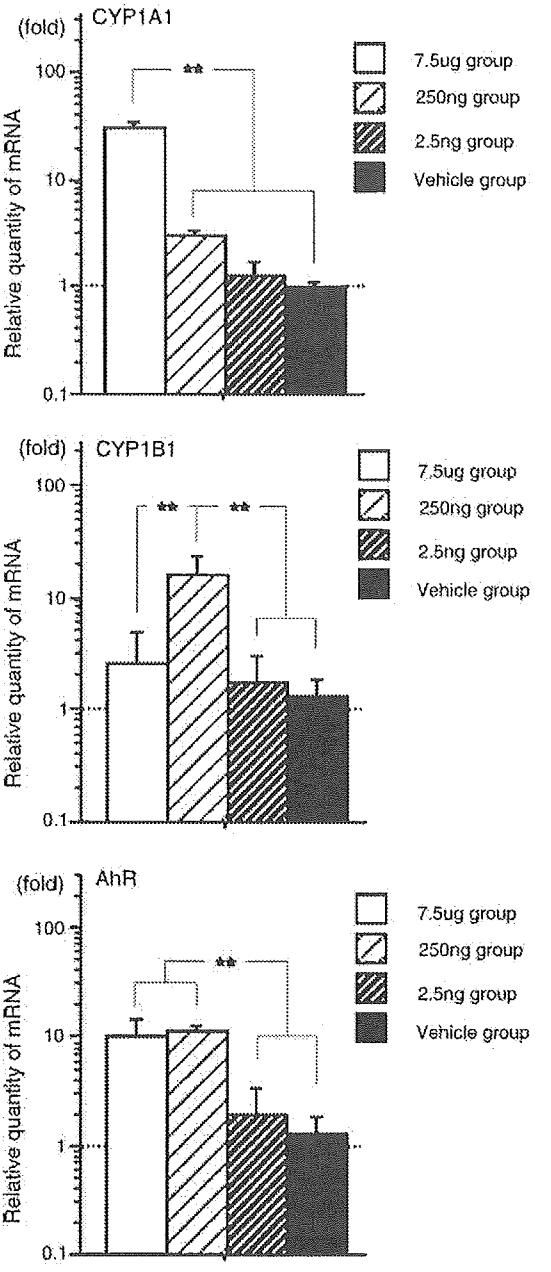

Fig. 4. Effect of prenatal exposure to PCB126 on CYP1A1 mRNA, CYP1B1 mRNA and AhR mRNA expression in DMBA-induced rat mammary carcinomas. The indicated mRNA levels were determined by real-time quantitative RT-PCR, with analysis using the standard curve method described in Section 2. Each level was normalized to that of the endogenous housekeeping gene control GAPDH in each tissue as described in Section 2. Values represent mean ± S.D. (**) Scheffé's F-test, $p < 0.01$.

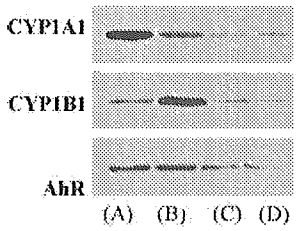

Fig. 5. Representative Western blots of CYP1A1, CYP1B1 and AhR of DMBA-induced rat mammary carcinomas after prenatal exposure to PCB126. The protein concentration was determined with a bicinchonic acid protein assay reagent kit (Pierce) with bovine serum albumin as a standard. Ten micrograms of microsome samples was applied for Western blotting analysis, and immunoreactive proteins were detected using the ECL Plus Western Blotting Detection system (Amersham Biosciences, Buckinghamshire, UK). Lane A, 7.5 μg group; lane B, 250 ng group; lane C, 2.5 ng group; and lane D, vehicle group. Higher expression of CYP1A1 and AhR was observed in the 7.5 μg group, and higher expression of CYP1B1 and AhR was observed in the 250 ng group.

CYP1B1 expression of the 250 ng group and/or a decrease in CYP1B1 expression of the 7.5 μg group. Although the PCB126 levels were only slightly increased in the 250 ng group, AhR levels were significantly increased in this group of animals, and the CYP1B1 observed in this group of rats might be, at least in part, associated with PCB126-induced AhR activation. However, there are possibilities that the higher expression of CYP1B1 in the 250 ng group is mediated by an as yet undefined endogenous AhR ligand or by factors capable of activating AhR in the absence of a nominal ligand (Trombino et al., 2000). Further study is required concerning the induction mechanism of CYP1B1 in the mammary carcinomas of the 250 ng group. Meanwhile it makes even less sense that there is a decrease in CYP1B1 expression of the 7.5 μg group because it is well established that the specific response to exposure to PCBs is a higher CYP1 induction (Walker et al., 1999), and the mammary carcinomas of the 7.5 μg group in this study are possessing a markedly high level of PCB126 residues (Table 5).

On the other hand, CYP1A1 catalyzes a step in the formation of 2-hydroxylated E2 (2OH-E2) metabolites, which are less toxic and has been considered to be protective against mammary carcinogenicity (Hayes et al., 1996; Yager and Liehr, 1996; Mobley et al., 1999; Schumacher et al., 1999; Cavalieri et al., 2002). The rapid conversion of the 2OH-E2 to other metabolites and subsequent clearance hinder an accurate assessment of intrinsic carcinogenic, estrogenic or other biological properties of this catechol (Bradlow et al., 1995). Moreover, 2OH-E2 and other catechols have been shown to inhibit inactivation of 4OH-E2 by catechol *O*-methyltransferase-catalyzed methylation (Zhu and Liehr, 1993). Because the concentration of PCB126 in mammary carcinomas of the 7.5 μg group was 10 times higher than that of the vehicle group in this study, the higher expression of CYP1A1 observed in the 7.5 μg group might be due to a direct induction by PCB126 residues in cancer cells. Moreover, several in vivo and in vitro studies have shown that PCB126 possess antiestrogenic effects that reduce both cellular E2 secretion and E2 gene-mediated biological effects, and these mediate expression of CYP1A1 (Heimler et al., 1998; Petroff et al., 2000; Sarkar et al., 2000). The lower incidence of DMBA-induced mammary carcinogenesis observed in the 7.5 μg group might be partially mediated through a higher expression of CYP1A1 in the mammary carcinomas of this group.

Although AhR-mediated induction of CYP1 has been the most frequently studied consequence of AhR activation, recent studies have uncovered an association between AhR activation and the cell cycle (Sadhu et al., 1993; Ma and Whitlock, 1996; Hushka et al., 1998; Tian et al., 1999). Moreover, the inhibition of growth of a human breast cancer cell line in culture (MCF-7) was reported following AhR down-regulation (Merchant et al., 1993; Dohr and Abe, 1997; Cover et al., 1998), and AhR-deficient cells exhibit a decreased rate of cell proliferation because of a prolongation of cells in G1 (Ma and Whitlock, 1996; Weiss et al., 1996). In this study, the higher expression of AhR was observed in the mammary carcinomas of the 7.5 μg and 250 ng groups. Constitutive AhR activation suggested a possible role for continued AhR signaling in maintenance of carcinoma growth through dysregulation of the cell cycle.

Our datum suggests that regulation of the genes encoding E2-metabolizing enzymes, such as CYP1A1 and 1B1, might constitute an important aspect of the toxicity of prenatal exposure to PCB126 in DMBA-induced rat mammary carcinogenesis. Additional experiments are required to confirm that the constitutive CYP1B1 expression observed in this system is AhR-influenced and is present throughout tumorigenesis.

Acknowledgements

This study was supported by a Grant-in-Aid for High-Tech Research Center Project from the Ministry of Education, Science and Culture, Japan. The authors thank Katherine Ono for critical reading and editing the manuscript.

References

Bombick, D., Jankun, J., Tullis, K., Matsumura, F., 1988. 2,3,7,8-Tetrachlorodibenzo-*p*-dioxin causes increase in expression of c-erb-A and levels of protein-tyrosine kinases in selected tissues of responsive mouse strains. Proc. Natl. Acad. Sci. U.S.A. 85, 4158.

Borlak, J., Hock, A., Hansen, T., Richter, E., 2003. DNA adducts in cultures of polychlorinated biphenyl-treated human hepatocytes. Toxicol. Appl. Pharmacol. 188, 81–91.

Bradlow, H.L., Arcuri, F., Blasi, L., Castagnetta, L., 1995. Effect of serum albumin on estrogen metabolism in human cancer cell lines. Mol. Cell. Endocrinol. 115, 221–225.

Cavalieri, E.L., Balu, N., Saeed, M., Devanesan, P., 2002. Catechol *ortho*-quinones: the electrophilic compounds that form depurinating DNA adducts and could initiate cancer and other diseases. Carcinogenesis 23, 1071–1077.

Cover, C.M., Hsieh, S.J., Tran, S.H., Hallden, G., Kim, G.S., Bjeldanes, L.F., Firestone, G.L., 1998. Indole-3-carbinol inhibits the expression of cyclin-dependent kinase-6 and induces a G1 cell cycle arrest of human breast cancer cells independent of estrogen receptor signaling. J. Biol. Chem. 273, 3838–3847.

Dohr, O., Abe, J., 1997. Transforming growth factor-beta1 co-regulates mRNA expression of aryl hydrocarbon receptor and cell cycle regulating genes in human cancer cell lines. Biochem. Biophys. Res. Commun. 8, 86–91.

Dwivedy, I., Devanesan, P., Cremonesi, P., Rogan, E., Cavalieri, E., 1992. Synthesis and characterization of estrogen 2,3- and 3,4-quinones. Comparison of DNA adducts formed by the quinines versus horseradish peroxidase-activated catechol estrogens. Chem. Res. Toxicol. 5, 828–833.

Furth, J., Cliftonk, H., Gadsden, E.L., Buffet, R.F., 1956. Dependent and autonomous mammotropic pituitary tumors in rats; their somatrophic features. Cancer Res. 16, 608–616.

Han, X., Liehr, J.G., 1994. DNA single-strand breaks in kidneys of Syrian hamsters treated with steroidal estrogens: hormone-induced free radical damage preceding renal malignancy. Carcinogenesis 15, 997–1000.

Hayes, C.L., Spink, D.C., Spink, B.C., Cao, J.Q., Walker, N.J., Sutter, T.R., 1996. 17-beta-Estradiol hydroxylation catalyzed by human cyotchrome P450 1B1. Proc. Natl. Acad. Sci. U.S.A. 93, 9776–9781.

Heimler, I., Trewin, A.L., Chaffin, C.L., Rawlins, R.G., Hutz, R.J., 1998. Modulation of ovarian follicle maturation and effects on apoptotic cell death in Holtzman rats exposed to 2,3,7,8-tetrachlorodibenzo-*p*-dioxin (TCDD) in utero and lactationally. Reprod. Toxicol. 12, 69–73.

Henderson, B.E., Ross, R.K., Pike, M.C., 1991. Toward the primary prevention of cancer. Science 254, 1131–1138.

Huang, Z., Fasco, M.J., Figgi, H.L., Keyomarski, K., Kaminski, L.S., 1996. Expression of cytochrome P450 in human breast tissues and tumors. Drug Metab. Dispos. 24, 889.

Huggins, C., Grand, L.C., Brillantes, F.K., 1961. Mammary cancer induced by a single feeding of polynuclear hydrocarbons, and its suppression. Nature 189, 204–207.

Hunter, D., Hankinson, S., Ladn, F.C., Colditz, G., Manson, J., Willett, W., Speizer, F., Wolff, M., 1997. Plasma organochlorine levels and the risk of breast cancer. N. Engl. J. Med. 337, 1253–1258.

Hushka, L.J., Willams, J.S., Greenlee, W.F., 1998. Characterization of 2,3,7,8-tetrachlorodibenzofuran-dependant suppression and AH receptor pathway gene expression in the developing mouse mammary gland. Toxicol. Appl. Pharmacol. 152, 200–210.

IARC Working Group on the Evaluation of Carcinogenic Risks to Humans, 1997. Polychlorinated dibenzo-*para*-dioxins and polychlorinated dibenzofurans. IARC Monogr. Eval. Carcinog. Risks Hum. 69, 1–631.

Lemon, H.M., Heidel, J.R., Rodriguez-Sierra, J.F., 1992. Increased catechol estrogen metabolism as a risk factor for nonfamilial breast cancer. Cancer Res. 69, 457–465.

Li, J.J., Li, S.A., Oberley, T.D., Parsons, J.A., 1995. Carcinogenic activities of various steroidal and nonsteroidal estrogens in the hamster kidney: relation to hormonal activity and cell proliferation. Cancer Res. 55, 4347–4351.

Liehr, J.G., Ricci, M.J., Jefcoate, C.R., Hannigan, E.V., Hokanson, J.A., Zhu, B.T., 1995. 4-Hydroxylation of estradiol by human uterine myometrium and myoma microsomes: implications for the mechanism of uterine tumorigenesis. Proc. Natl. Acad. Sci. U.S.A. 92, 9220–9224.

Ma, Q., Whitlock, J.P., 1996. The aromatic hydrocarbon receptor modulates the Hepa 1c1c7 cell cycle and differentiated state independently of dioxin. Mol. Cell. Biol. 16, 2144–2150.

McKay, J., Melvin, W., Ah-See, A., Ewen, S., Greenlee, W., Marcus, C., Burke, M., Murray, G., 1995. Expression of cytochrome P450 CYP1B1 in breast cancer. FEBS Lett. 374, 270–272.

Merchant, M., Krishnan, V., Safe, S., 1993. Mechanism of action of alpha-naphthoflavone as an Ah receptor antagonist in MCF-7 human breast cancer cell. Toxicol. Appl. Phramacol. 120, 53–63.

Mobley, J.A., Bhat, A.S., Bruggemeier, R.W., 1999. Measurement of oxidative DNA damage by catechol estrogens and analogues in vivo. Chem. Res. Toxocol. 12, 270–277.

Murray, G.L., Taylor, M.C., McFadyen, M.C., MacKay, J.A., Greenlee, W.F., Burke, M.D., Melvin, W.T., 1997. Tumor-specific expression of cytochromes P450 CYP1B1. Cancer Res. 57, 3026–3031.

Muto, T., Wakui, S., Imano, N., Nakaaki, K., Hano, H., Furusato, M., Masaoka, T., 2001. In-utero and lactational exposure of 3,3′,4,4′,5-pentachlorobiphenyl modulates dimethylbenz[*a*]anthracene-induced rat mammary carcinogenesis. J. Toxicol. Pathol. 14, 213–224.

Nandi, S., Guzman, R.C., Yang, J., 1995. Hormones and mammary carcinogenesis in mice, rat, and humans: a unifying hypothesis. Proc. Natl. Acad. Sci. U.S.A. 92, 3650–3657.

Newbold, R.R., Liehr, J.G., 2000. Induction of uterine adenocarcinoma in CD-1 mice by catechol estrogens. Cancer Res. 60, 235–237.

Petroff, B.K., Gao, X., Rozman, K.K., Terranova, P.F., 2000. Interaction of estradiol and 2,3,7,8-tetrachlorodibenzo-*p*-dioxin (TCDD) in an ovulation model: evidence for systemic potentiation and local ovarian effects. Reprod. Toxicol. 14, 247–255.

Rowlands, J., He, L., Hakkak, R., Roins, M., Badger, T., 2001. Soy and whey proteins downregulate DMBA-induced liver and mammary gland CYP1 expression in female rats. Nutr. Cancer 131, 109–134.

Russo, J., Russo, I.H., 2000. Atlas and histologic classification of tumors of the rat mammary gland. J. Mammary Gland Biol. Neoplasia 5, 187–200.

Sadhu, D., Merchant, M., Safe, S., Ramos, K., 1993. Modulation of protooncogene expression in rat aortic smooth muscle cell by benzo[*a*]pyrene. Arch. Biochem. Biophys. 300, 124–131.

Safe, S., Krishnan, V., 1995. Cellular and molecular biology of aryl hydrocarbon (Ah) receptor-mediated gene expression. Arch. Toxicol. 17, 99–115.

Sarkar, S., Jana, N.R., Yonemoto, J., Tohyama, C., Sone, H., 2000. Estrogen enhances induction of cytochrome P-4501A1 by 2,3,7,8-tetrachlorodibenzo-*p*-dioxin in liver of female Long-Evans rats. Int. J. Oncol. 16, 141–147.

Sasaki, M., Kaneuchi, M., Fujimoto, S., Tanaka, Y., Dahiya, R., 2003. CYP1B1 gene in endometrial cancer. Mol. Cell. Endocrinol. 202, 171–176.

Schumacher, G., Kataoka, M., Roth, J.A., Mukhopadhyay, T., 1999. Potent antitumor activity of 2-methoxyestradiol in human pancreatic cancer cell lines. Clin. Cancer Res. 5, 493–499.

Shan, L., He, M., Yu, M., Qiu, C., Lee, N.H., Liu, E.T., Snyderwine, G., 2002. cDNA microarray profiling of rat mammary gland carcinomas induced by 2-amino-1-methyl-6-phenylimidase[4,5-*b*]pyridine and 7,12-dimethylbenz[*a*]anthracene. Carcinogenesis 23, 1561–1568.

Tanabe, S., Tatsukawa, R., Phillips, D., 1987. Mussels as bioindicators of PCB pollution: a case study on uptake and release of PCB isomers and congeners in green-lipped mussels (*Perna viridis*) in Hong Kong waters. Environ. Pollut. 47, 41–62.

Tang, Z., Treilleux, L., Brown, M., 1997. A transcriptional enhancer required for the differential expression of the human estrogen receptor in breast cancer. Mol. Cell. Biol. 17, 1274–1280.

Tharappel, J., Lee, E., Robertson, L., Spear, B., Glauert, H., 2002. Regulation of cell proliferation, apoptosis, and transcription factor activities during the promotion of liver carcinogenesis by polychlorinated biphenyls. Toxicol. Appl. Pharmacol. 179, 172–184.

Thenot, S., Charpin, M., Bonnet, S., Cavailles, V., 1999. Estrogen receptor cofactors expression in breast and endometrial human cancer cells. Mol. Cell. Endocrinol. 156, 85–93.

Tian, Y., Ke, S., Denison, M.S., Rabson, A.B., Gallo, M.A., 1999. Ah receptor and NF-kB interactions, a potential mechanism for dioxin toxicity. J. Biol. Chem. 274, 510–515.

Trombino, A.F., Near, R., Matulka, R.A., Yang, S., Hafer, L.J., Toselli, P.A., Kim, D.W., Rogers, A.E., Sonenshein, G.E., Sherr, D.H., 2000. Expression of the aryl hydrocabon receptor/transcription factor (AhR) and AhR-regulated CYP1 gene transcripts in a rat model of mammary tumorigenesis. Breast Cancer Res. Treat. 63, 117–131.

van den Berg, M., Birnbaum, L., Bosveld, A.T.C., Brunstrom, B., Cook, P., Feely, M., Giesy, J.P., Hanberg, A., Hasegawa, R., Kennedy, S.W., Kubiak, T., Larsen, J.C., Rolaf van Leeuwen, F.X., Liem, A.K.D., Nolt, C., Peterson, R.E., Poellinger, L., Safe, S., Schrenk, D., Tillitt, D., Tysklind, M., Younes, M., Waern, F., Zacharewski, T., 1998. Toxic equivalency factors (TEFs) for PCBs, PCDDs, PCDFs for human and wildlife. Environ. Health Perspect. 106, 775–792.

Walker, N., Portier, C., Lax, S., Crofts, F., Li, Y., Lucier, G., Sutter, T., 1999. Characterization of the dose-response of CYP1B1, CYP1A1, and CYP1A2 in the liver of female Sprague–Dawley rats following chronic exposure to 2,3,7,8-tetrachlorodibenzo-*p*-dioxin. Toxicol. Appl. Pharmacol. 154, 279–286.

Weinberg, R.A., 1996. How cancer arises. Sci. Am. 275, 62–70.

Weiss, C., Kolluri, S.K., Kiefer, F., Gottlicher, M., 1996. Complementation of Ah receptor deficiency in hepatoma cells: negative feedback regulation and cell cycle control by Ah receptor. Exp. Cell Res. 226, 154–163.

Yager, J.D., Liehr, J.G., 1996. Molecular mechanisms of estrogen carcinogenesis. Annu. Rev. Pharmacol. Toxicol. 36, 203–232.

Zhu, B.T., Liehr, J.G., 1993. Inhibition of the catechol-*O*-methyltransferase-catalyzed *O*-methylation of 2- and 4-hydroxyestradiol by catecholamine: implications for the mechanism of estrogen-induced carcinogenesis. Arch. Biochem. Biophys. 304, 248–256.

Virchows Arch (2006) 448: 142–150
DOI 10.1007/s00428-005-0063-7

ORIGINAL ARTICLE

Kuniaki Nakanishi · Hirotaka Matsuo · Yoshikatsu Kanai · Hitoshi Endou · Sadayuki Hiroi · Susumu Tominaga · Makio Mukai · Eiji Ikeda · Yuichi Ozeki · Shinsuke Aida · Toshiaki Kawai

LAT1 expression in normal lung and in atypical adenomatous hyperplasia and adenocarcinoma of the lung

Received: 27 April 2005 / Accepted: 15 August 2005 / Published online: 21 September 2005

Abstract No previous study has investigated neutral large amino acid transporter type 1 (LAT1) in normal lung cells, or in atypical adenomatous hyperplasia(s) (AAH) and nonmucinous bronchioloalveolar carcinoma(s) (NMBAC) of the lung. The authors examined: (1) the levels of *LAT1* mRNA/*glyceraldehyde-3-phosphate dehydrogenase* (*GAPDH*) mRNA in 41 normal lung tissues and 34 NMBAC using semiquantitative reverse transcription–polymerase chain reaction; (2) LAT1 mRNA and protein expressions in 35 normal lung tissues, 34 AAH (11 lesions were interpreted as low-grade AAH and 23 as high-grade AAH), and 43 NMBAC using in situ hybridization and immunohistochemistry; and (2) the association of the incidences of LAT1 mRNA and protein expressions with cell proliferation in these lesions. The level of *LAT1* mRNA/*GAPDH* mRNA (1) tended to be higher in NMBAC (12.0± 8.1) than in normal lung tissues (1.0±0.2), and (2) covered a much wider range (from 0 to 276) in NMBAC than in normal lung tissues (from 0 to 5.8), with six NMBAC having values higher than 7.0, while 5.8 was the highest value detected in normal lung tissues. In peripheral normal lung tissues, *LAT1* mRNA and protein were detected in bronchial surface epithelial cells and alveolar macrophages (but not in nonciliated bronchiolar epithelial cells, or in alveolar type I or type II cells). In bronchial surface epithelial cells, LAT1 protein appeared to be of a nodular type, which was considered to be a nonfunctional protein pattern. The incidences of positive expressions for *LAT1* mRNA and protein were 54.5 and 27.3% in low-grade AAH, 65.2 and 52.2% in high-grade AAH, and 65.1 and 79.1% in NM BAC, respectively. In the case of LAT1 protein expression, significant differences could be shown between total (low-grade plus high-grade) AAH and NMBAC, and between low-grade AAH and NMBAC. Thus, in terms of the incidence of LAT1 protein expression, high-grade AAH appeared intermediate between low-grade AAH and NMBAC. The Ki-67 labeling index (a cell proliferation score) was significantly higher in those AAH and NMBAC that were LTA1-protein-positive than in their LAT1-protein-negative counterparts. In conclusion, LAT1 expression may increase with the upregulation of metabolic activity and cell proliferation in high-grade AAH and NMBAC.

Keywords Atypical adenomatous hyperplasia
Pulmonary bronchioloalveolar carcinoma · Amino acid transporter · LAT1

K. Nakanishi (✉) · S. Hiroi · S. Tominaga · T. Kawai
Department of Pathology,
National Defense Medical College,
Tokorozawa, 359-8513, Japan
e-mail: nknsknak@ndmc.ac.jp
Tel.: +81-42-9951505
Fax: +81-42-9965192

H. Matsuo
Department of Physiology,
National Defense Medical College,
Tokorozawa, 359-8513, Japan

Y. Kanai · H. Endou
Department of Pharmacology and Toxicology,
School of Medicine, Kyorin University,
Tokyo, 181-8611, Japan

M. Mukai
Division of Diagnostic Pathology,
School of Medicine,
Keio University,
Tokyo, 160-8582, Japan

E. Ikeda
Department of Pathology,
School of Medicine,
Keio University,
Tokyo, 160-8582, Japan

Y. Ozeki
Department of Surgery,
National Defense Medical College,
Tokorozawa, 359-8513, Japan

S. Aida
Department of Laboratory Medicine,
National Defense Medical College,
Tokorozawa, 359-8513, Japan

Introduction

Nonmucinous bronchioloalveolar carcinoma(s) (NMBAC) of the lung is one of the major histological types of lung adenocarcinoma [24]. In the 1999 *World Health Organization international histologic classification of tumours* [25], it is defined as an adenocarcinoma with a pure bronchioloalveolar growth pattern and with no evidence of stromal, vascular, or pleural invasion. However, its histogenesis is not well-understood. Atypical adenomatous hyperplasia(s) (AAH) of the lung, which is classified among preinvasive lesions in the World Health Organization classification of lung and pleural tumours [25], is a proliferation of alveolar epithelial cells and is usually found incidentally in lungs surgically resected for lung cancer, predominantly in patients with adenocarcinoma.

Facilitated diffusion and active transport are responsible for the transport of substances such as glucose and amino acids. System L-amino acid transport mediates sodium-independent uptake of nonpolar branched-chain or aromatic neutral amino acids and is the major route by which mammalian cells take up nutritionally essential amino acids from extracellular fluids [2, 3, 5, 6]. Indeed, system L-amino acid transport plays a critical role in the absorption of amino acids by the intestine, kidney, and placenta. Recently, genes encoding proteins responsible for system L-amino acid transport have been cloned, and large amino acid transporter type 1 (LAT1) is the first member of the system L-amino acid transporter family to be identified [7, 10]. LAT1 requires covalent association with the heavy chain of 4F2 cell surface antigen (4F2hc) for its functional expression in plasma membrane [22]. Previous studies have shown LAT1 to be highly expressed in proliferating tissues, many tumor cell lines, and primary human tumors, but to be at barely detectable levels in adult tissues (except the brain, testis, and placenta), while 4F2hc is ubiquitous [2, 3, 5, 6, 8, 19–21, 23, 26]. Furthermore, overexpression of LAT1 in hepatocytes has been found to enhance their growth, leading Campbell and Thompson [1] to suggest that LAT1 may play an important role in cell growth. However, no study has yet investigated LAT1 expression in normal lung cells, or in AAH and NMBAC of the lung.

In this study, we took the opportunity to examine the expression of LAT1 mRNA and protein in normal lung cells, as well as in AAH and NMBAC. We investigated: (1) whether distributions of LAT1 mRNA and protein would be revealed in normal lung tissues; (2) whether LAT1 mRNA might be produced in normal lung tissues and NMBAC; (3) whether incidences of LAT1 mRNA and protein expressions might differ among normal lung tissues, precancerous lesions, and peripherally located adenocarcinomas; and (4) whether incidences of LAT1 mRNA and protein expressions would show associations with cell proliferation in these lesions. To those ends, we measured the levels of *LAT1* mRNA/*glyceraldehyde-3-phosphate dehydrogenase* (*GAPDH*) mRNA in 41 normal lung tissues and 34 NMBAC (measuring 30 mm or less in the greatest diameter) using a real-time reverse transcription–polymerase chain reaction (RT-PCR) approach. Furthermore, we examined the expressions of LAT1 mRNA and protein as well as cell proliferation index in 35 normal lung tissues, 34 AAH, and 43 bronchioloalveolar carcinomas (measuring 20 mm or less in the greatest diameter) using in situ hybridization and immunohistochemical approaches. Our goal was to obtain a better understanding of the relation of LAT1 expression to metabolic activity in normal lung cells, AAH, and NMBAC.

Materials and methods

From 1980 to 2002, the surgical pathology services of the National Defense Medical College Hospital (Tokorozawa, Japan) and the Keio University Hospital (Tokyo, Japan) received fresh frozen tissues of 41 normal lungs (resected from 41 patients with lung cancer) and 34 NMBAC of the lung (resected from 34 patients; measuring 30 mm or less in the greatest diameter), and also paraffin-embedded specimens of 34 AAH of the lung (resected from 19 patients) and 43 NMBAC of the lung (resected from 43 patients; measuring 20 mm or less in the greatest diameter). Of the 34 AAH lesions, 23 were interpreted as high-grade based on the findings of increased cellularity and cytological pleomorphism [14–17].

RT-PCR

Total mRNAs were obtained from the 41 normal lung tissues and 34 NMBAC (measuring 30 mm or less in the greatest diameter) that were available. Total RNA was isolated using acid guanidinium isothiocyanate–phenol–chloroform extraction and ethanol precipitation [4]. RT-PCR was performed using an amplification reagent kit (TaqMan EZRT-PCR kit; Applied Biosystems, Alameda, CA) with *LAT1* or *GAPDH* primers, as previously reported [18]. The *LAT1* and *GAPDH* primers were synthesized by an automated DNA synthesizer. The sense and antisense sequences of the *LAT1* primers were 5′-GTG ACG CTG GTG TAC GTG CT-3′ and 5′-GGG TGG ATC ATG GAG AGG AT-3′, respectively, while the sequence of the Taq Man probe was 5′-CTC CGT CAA TGG GTC CCT GTT CAC AT-3′. The cDNA amplification product was predicted to be a 251-bp fragment from positions 918 to 1,168 in the cDNA of *LAT1*. Primers were also synthesized to amplify the cDNA encoding *GAPDH*, a constitutively expressed gene, as a control. In the case of *GAPDH*, the sequences of the primers and TaqMan probe used were 5′-GAA GGT GAA GGT CGG AGT C-3′ (sense), 5′-GAA GAT GGT GAT GGG ATT TC-3′ (antisense), and 5′-CAA GCT TCC CGT TCT CAG CC-3′ (TaqMan probe). Both TaqMan probes were labeled at the 5′ end with the reporter dye molecule 6-carboxyfluorescein and at the 3′ end with the quencher dye 6-carboxytetramethylrhodamine. The re-